Metallomics

Accepted Manuscript

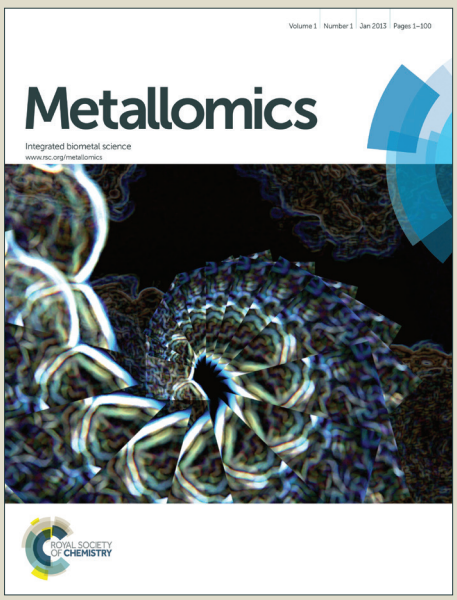

ROYAL SOCIETY OF CHEMISTRY

www.rsc.org/metallomics

ZnT-1 extrudes zinc from mammalian cells functioning as a Zn^{2+}/H^{+} exchanger

Eden Shusterman[1*], Ofer Beharier[1*], Levy Shiri[1], Raz Zarivach[2], Yoram Etzion[1], Craig R. Campbell[3], Il-Ha Lee[3], Ken Okabayashi[3,5], Anuwat Dinudom[3], David I. Cook[3], Amos Katz[4], Arie Moran[1,3]

[1]Department of Physiology and Cell Biology, Faculty of Health Sciences, Ben Gurion University of the Negev, Israel. [2]Department of Life Sciences, Faculty of Natural Sciences, Ben Gurion University of the Negev, Israel. [3]Discipline of Physiology, The Bosch Institute, Faculty of Medicine, The University of Sydney, Sydney, NSW 2006, Australia. [4]Department of Cardiology, Barzelai Medical University Center, Ashkelon, Israel. [5]Department of Veterinary Medicine, College of Bioresource Sciences, Nihon University, Japan.

* The first two authors contributed equally

Abstract

ZnT-1 is a Cation Diffusion Facilitator (CDF) family protein, and is present throughout the phylogenetic tree from bacteria to humans. Since its original cloning in 1995, ZnT-1 has been considered to be the major Zn^{2+} extruding transporter, based on its ability to protect cells against zinc toxicity. However, experimental evidence for ZnT-1 induced Zn^{2+} extrusion was not convincing. In the present study, based on the 3D crystal structure of the ZnT-1 homologue, YiiP, that predicts a homodimer that utilizes the H^{+} electrochemical gradient to facilitate Zn^{2+} efflux, we demonstrate ZnT-1 dependent Zn^{2+} efflux from HEK 293T cells using FluoZin-3 and Fura 2 with single cell microscope based fluorescent imaging. ZnT-1 facilitates zinc efflux in a sodium-independent, pH-driven and calcium-sensitive manner. Moreover, substitution of two amino acids in the putative zinc binding domain of ZnT-1 led to nullification of Zn^{2+} efflux and rendered the mutated protein incapable of protecting cells

against Zn^{2+} toxicity. Our results demonstrate that ZnT-1 extrudes zinc from mammalian cells by functioning as a Zn^{2+}/H^{+} exchanger.

Introduction

Zinc ions play an essential role in mammalian development and function. Zinc deficiency severely affects embryonic development [1-3] and, later in life, zinc plays an important role in the proper function of multiple systems [4]. At the cellular level, zinc activates transcription factors by interacting with specific zinc fingers, thus controlling the expression of genes and proteins involved, for example, in cell division, development and differentiation [4]. In mammalian cells, Zn^{2+} is distributed along a steep electrochemical gradient that may exceed 6 orders of magnitude across the plasma membrane [5-8]. An imbalance in zinc homeostasis, leading to an excess in intracellular zinc, has toxic effects. For example, a rapid rise in extracellular zinc levels is considered to be a major cause of neuronal damage during brain ischemia, seizures and trauma [6, 9, 10]. Hence, intracellular free zinc levels need to be tightly regulated, with intracellular chelatable zinc being maintained in the nanomolar range.

Numerous mechanisms regulate cellular zinc levels, including a variety of intracellular proteins, such as metallothioneins and zinc chelators, that act as buffers [8]. As a charged ion, zinc does not freely diffuse through the plasma membrane but rather enters cells through channels and transporters of divalent cations [11]. In this way, the members of the Zip family of transporters function to increase cytosolic zinc concentration [8, 11-16]. Conversely, members of the ZnT family of transporters deplete cytosolic zinc by sequestering zinc into cellular compartments or directly transporting zinc from the cytosol to the extracellular milieu [8, 11, 13, 14].

ZnT-1 (SLC30A1) was cloned almost two decades ago and was the first member of the ZnT family to be identified [17]. Based on its protective effect against zinc toxicity, its ability to transport radioactive zinc to the extracellular medium, and its localization to the plasma membrane, Palmiter et. al. proposed that ZnT-1 functions as a zinc extruder [17]. These initial findings were later reinforced by data showing that: 1) ZnT-1 protects a variety of cell types from zinc toxicity [18-23], 2) Other ZnTs that structurally resemble ZnT-1 sequester zinc into intracellular compartments [11], 3) In other ZnTs, zinc transport is dependent upon an H^{+} driving force [14], and 4) ZnT-5 contains a zinc binding domain critical for zinc transport [24]. However, evaluation of the activity of ZnTs was performed for ZnT-5 which is expressed in

intracellular compartments. This limitation has impeded direct testing of both the effect of ions such as H^+ and Ca^{2+} on the activity of the transporters, and their ability to transport Zn^{2+} against a gradient. Hence, despite continuing investigations, the mechanism underlying ZnT-1 mediated zinc transport has yet not been directly elucidated.

The ZnT protein family belongs to the Cation Diffusion Facilitator (CDF) protein family that contributes to transport of a variety of divalent ions, including zinc, manganese and iron [25]. Currently, the only existing high resolution structure of a full CDF protein is of the bacterial zinc extruder YiiP from *E. coli* [26]. The YiiP structure shows a homodimeric membrane organization in which each monomer has six integral membrane helices with a buried conserved ion binding site within the membrane domain [26]. Like many other secondary active transporters, YiiP facilitates the efflux of metals such as iron and zinc by utilizing the hydrogen ion gradient [27]. Following the resolution of the YiiP structure, Lu showed that CDF acts as a Zn^{2+} /H exchanger [26, 28]. That the mammalian YiiP homologue, ZnT-5, functions as an Zn^{2+}/H^+ exchanger was demonstrated by fluorescent imaging experiments which documented a decline in the cytosolic Zn^{2+} concentration and its sequestration into intracellular vesicles [24].

In the present work, we have investigated the zinc extruding activity of ZnT-1, its driving force, and ion dependence, by monitoring zinc efflux from mammalian cells utilizing FluoZin-3 and Fura-2. We demonstrate that the facilitated zinc efflux induced by ZnT-1 against a zinc gradient is sodium-independent, pH-driven and calcium-sensitive. Site directed mutagenesis in the putative zinc binding domain abolished ZnT-1 mediated zinc efflux and the ability of ZnT-1 to protect cells against zinc toxicity, supporting the notion that this domain is indeed critical for the function of ZnT-1 as a zinc extruder.

Material and Methods

Cell culture and transfection

Human embryonic kidney (HEK 293T) cells were maintained in high glucose Dulbecco's modified Eagle's medium supplemented with (v/v) 1% penicillin/streptomycin, 1% L-glutamine, and 10% fetal bovine serum at 37^{o}C in a humidified 5% CO_2 incubator. 24 h before transfection, the cells were subcultured onto glass cover slips in 24 well culture dishes and seeded to reach 50–60% confluence. HEK 293T cells were transfected utilizing Lipofectamine 2000, according to the manufacturer's instructions. Cell culture reagents were purchased from Life Technologies, Australia or Bet Haemek, Israel.

Plasmids used for expression of ZnT-1 WT, ZnT-1 truncations, and ZnT-1 Mutants in HEKT293 cells

Two plasmids were used for the expression of ZnT-1 wild type (WT): ZnT-1-pEYFP-N1 and ZnT-1-pECFP-N1 (rat ZnT-1 tagged with YFP or CFP at the C-terminal).

Three plasmids were used for the expression of ZnT-1 truncations:

1) ZnT-1ΔCT, a vector containing a truncated form of ZnT-1 with a deletion of 156 amino acids at the C-terminal segment, 2) ZnT-1CT, a vector containing the C-terminal segment of ZnT-1 3) The ZnT-1 mutant ZnT-1 H43A D254A containing a double point mutation at 43 (Histidine mutated to Alanine) and at 254 (Aspartate mutated to Alanine) tagged either with myc or with pEYFP at the C-terminal.

Plasmid construction

ZnT-1-pEYFP-N1 and ZnT-1-pECFP-N1 were cloned by transfer of full length ZnT-1 from the ZnT-1-pJJ19 plasmid [29], upstream of EYFP or ECFP in pEYFP-N1 or pECFP-N1, respectively (Clontech; enhanced yellow or cyan fluorescent proteins).

ZnT-1minusCT was constructed as follows: the pJJ19 plasmid was digested by EcoRV producing a ZnT-1dCT fragment and the pJJ19 backbone. Both fragments were isolated and the pJJ19 backbone was digested again using HindIII, cutting off the remaining C-terminal segment from the backbone. Klenow polymerase was then used to blunt the ends of the pJJ19 backbone. Thereafter, the ZnT-1minusCT fragment and pJJ19 backbone were ligated, forming the ZnT-1minusCT plasmid.

ZnT-1CT was constructed as follows: The CT fragment was subcloned by PCR amplification of the ZnT-1 C-terminal domain from the ZnT-1-pJJ19 vector utilizing the following primers: Forward: AAGCTTATGCCACTGCTCAAGGAGTCCGC and Reverse: AAAAATCCCTCGAGGTCGACTAGAC. The PCR product (525 bp) was then ligated into the pcDNA vector between the HindIII and XhoI sites followed by sequence verification. ZnT-1CT-pEYFP-N1 was subcloned by transfer of full length ZnT-1CT from the ZnT-1CT plasmid, upstream of EYFP in pEYFP-N1.

ZnT-1D254A_H43A was constructed as follows: site-directed mutagenesis was performed on the ZnT-1D254A plasmid using again the KAPA HiFi kit (KAPA Biosystems). The

following primer was utilized: ZnT-1D254A_H43A ,ATGCTGTCCGACTCCTTC**GCC**ATGCTGTCGGACGTGCT, as well as a primer composed of the reverse and complementary sequences.

ZnT-1D254A_H43A-pEYFP-N1 and ZnT-1D254A_H43A-pECFP-N1 were constructed as follows: ZnT-1D254A_H43A plasmid was digested by HindIII producing ZnT-1D254A_H43A fragment. pEYFP-N1 and pECFP-N1 plasmids were also digested by HindIII producing pEYFP-N1 and pECFP- N1 backbones, respectively. All fragments and backbones were isolated and ligated, forming the plasmids above.

Zn^{2+} efflux measurements

Coverslips (No. 1, 10 mm diam.; Thermo Fischer Scientific) with cells transfected with the appropriate plasmids were loaded with either FluoZin-3 AM or Fura-2 AM as previously described [23]. Briefly, slides were washed in Calcium Ringer (CaR) solution (in mM: NaCl 120, KCl 5.4, Na-HEPES 5, H-HEPES 5, Glucose 10, $CaCl_2$ 1, $MgCl_2$ 0.8, adjusted to pH 7.4), and then incubated in the same solution containing 5 µM of the fluorescent dye and 0.05% pluronic acid and 0.1% albumin, for 20 min at room temperature, followed by incubation in the wash solution for an additional 15 min (CaR with 0.1% albumin). The slides were then mounted on a microscope stage (Zeiss Axiovert 200) and intracellular zinc was monitored using an excitation wavelength of 488 nm and read at 530 nm emission for FluoZin-3, or excited at 340 nm and 380 nm and monitored at 530 nm for Fura-2 loaded cells. Transfected cells were identified by their fluorescent tags (CFP and YFP for FluoZin-3 and Fura-2, respectively). Intracellular Zn^{2+} was measured under constant perfusion. Following a baseline period, the cells were loaded with zinc by perfusion with CaR solution containing 5 µM pyrithione and 1 µM $ZnCl_2$. Efflux was initiated by superfusing the cells (by gravity) with the appropriate solution. Efflux rate was determined by a linear fit to the initial reduction in fluorescence. All efflux rates were expressed as the percent of control cells transfected with ZnT-1 and washed with normal Ringer's solution.

Zinc toxicity assay of cultured HEK293T cells

HEK 293T cells were subcultured into 24-well plates and seeded to reach 60–70% confluence. The following day the cells were transfected utilizing a calcium phosphate transfection protocol. The cell medium was replaced 24 h after transfection with fresh medium lacking Phenol Red and supplemented with (v/v) 1% penicillin/streptomycin, 1% L-

glutamine, and 1% bovine serum albumin (all from Bet-Haemek, Israel). One hour after medium replacement, cells were treated with zinc by addition of $ZnSO_4$ to the cells for 24 hours at a final concentration ranging from 150 to 400 µM. Cell death was assessed by measuring lactate dehydrogenase (LDH) using a cytotoxicity detection kit (Roche, Mannheim, Germany) according to the manufacturer's instructions. LDH release was expressed as the ratio between LDH released following the zinc treatment protocol (LDH Zn) and the total LDH measured after lysis of all cells by addition of triton lysis buffer to the medium (LDH T), as previously described[30]. LDH release was expressed as the ratio between the values observed in the Zn^{2+} exposed cells and the matched non Zn^{2+} treated control group.

ZnT-1 Homology model preparation

An hZnT-1 model was built based on the template structure (3H90) with the Swiss-model server (http://swissmodel.expasy.org/) in an automatic mode. The automatic mode compares all available structures and includes sequence analysis to allow the best model with a correct position for conserved residues. Images were prepared by the pyMOL program [31].

Statistical Analysis

Values are expressed as means ± SE. Student's *t*-test was used to determine statistical significance. Statistical significance was set at $p < 0.05$.

Results

In order to determine ZnT-1 mediated zinc efflux, we loaded HEK 293T cells with Zn^{2+} by superfusing them with Ringer's solution containing 5 µM pyrithione and 1 µM $ZnCl_2$. Intracellular Zn^{2+} increased rapidly, as measured by either FluoZin-3 or Fura-2, in both control cells and cells transfected with ZnT-1. Under these experimental conditions, the observed increase in fluorescence is fully due to an increase in intracellular Zn^{2+} since the application of the membrane-permeate Zn^{2+} chelator, TPEN (50 µM), totally eliminates the increase in fluorescent signal [32]. When the zinc loaded cells were washed with CaR solution containing 100 µM EGTA, intracellular Zn^{2+} gradually decreased in ZnT-1 transfected cells (Figure 1A and 1B) but not in the matched control cells that had been transfected with pcDNA. Zinc efflux rate was determined from the slope of the linear part of the measured fluorescent decrease during the wash with CaR. The bar graph shown in Figure 1C summarizes the rates of zinc efflux in control cells relative to ZnT-1-transfected cells in 10

independent experiments. It shows that while no significant efflux was measured in control cells, ZnT-1 expression led to marked Zn^{2+} efflux from the cells ($p<0.001$).

Searching for the ion dependency of ZnT-1 mediated Zn^{2+} efflux, we next measured the calcium dependence of ZnT-1 induced Zn^{2+} efflux. No Zn^{2+} efflux is observed when zinc loaded cells are washed with calcium-free medium (CaF-■) and efflux was started when the cells were washed with calcium-containing Ringer's solution (CaR-●) (Figure 2A). The zinc extruding activity of ZnT-1 is independent of sodium, since ZnT-1 mediated Zn^{2+} efflux is observed when cells are washed with calcium-containing Ringer's solution in which sodium is substituted with N-methyl-D-glucamine (NMG-CaR). This is consistent with the finding in figure 2A in which no Zn^{2+} efflux is seen when the wash does not contain calcium (NMG-CaF) (Figure 2B). Furthermore, Mg^{2+}, which at 2 mM does not inhibit ZnT-1 mediated Zn^{2+} efflux, cannot substitute for Ca^{2+} in supporting Zn^{2+} efflux (Figure 2C). Taken together these findings are consistent with the notion that the stimulatory effect of calcium ions on Zn^{2+} efflux is not due to nonspecific effects of divalent ions. The calcium concentration dependence of ZnT-1 mediated Zn^{2+} efflux (Figure 2D) is consistent with cooperative activity of calcium, since fitting the data to a Hill plot yields a Hill coefficient of 1.7.

Members of the CDF protein family are known to facilitate transport of heavy and transition metal ions such copper, iron, manganese and zinc. Many of these transporters utilize the pH gradient for extruding divalent cations from the cytosol to the extracellular fluids or for sequestering the metals into intracellular compartments [11]. We found that, like other members of the ZnT family, ZnT-1 extrudes zinc across the plasma membrane of HEK 293T cells by utilizing the electrochemical gradient of hydrogen ions (Figure 3A). The H^+ concentration dependence of the transport activity shows that the pH dependency of ZnT-1 activity is within the physiological range as the apparent Km achieved by fitting the experimental points to a Michaelis-Menten equation corresponded to a pH= 6.8±0.2. To investigate the possibility that $[H^+]$ serves as a regulator rather than as the driving force, we investigated the rate of Zn^{2+} efflux in cells in which intracellular pH was either alkalinized or acidified prior to the onset of efflux. As expected from a pH driven transport process, Zn^{2+} efflux rates were significantly reduced or augmented when cytosolic pH was acidified ($p<0.001$; perfusing with 30 mM sodium butyrate) or alkalinized ($p<0.03$; perfusing with 30 mM ammonium chloride), respectively (Figure 3B). These findings are consistent with Zn^{2+} efflux being

driven by the electrochemical gradient of [H^+] rather than pH having a modulatory role on ZnT-1 activity.

As a protector against Zn^{2+} toxicity, it was predicted that ZnT-1 would mediate Zn^{2+} efflux against a Zn^{2+} concentration gradient. In accordance with this prediction, cells transfected with ZnT-1 and loaded with Zn^{2+} were able to extrude Zn^{2+} into a washing solution containing 10 μM Zn^{2+} (Figure 4A). The dependency of ZnT-1 mediated Zn^{2+} extrusion on extracellular Zn^{2+} concentration was assessed by measuring the ZnT-1 mediated Zn^{2+} efflux as a function of extracellular Zn^{2+} during the washing period. ZnT-1 was observed to extrude Zn^{2+} against more than a 100 fold zinc gradient (Figure 4B)

As originally reported by Palmiter and Findley [17], ZnT-1 protects HEK 293T cells against zinc toxicity, as evaluated by the release from the cytosol of the large molecule Lactate Dehydrogenase (LDH) - Figure 5A. In this study [17], neither the C-Terminal (CT) truncated form, nor the C-Terminal by itself, was found to protect cells against zinc toxicity. To further define the structural requirements of zinc transport by ZnT-1, we used the published molecular structure of YiiP to build a three dimensional homology model of ZnT-1. This model predicted that Asp254 and His43 in ZnT-1 should function as key residues in the putative zinc binding domain of ZnT-1 (Figure 5B). Indeed, when these two residues were substituted with alanine, ZnT-1 lost its ability to protect cells against zinc toxicity (Figure 5C) This observation is supported by the finding that the mutated ZnT-1 also lost its ability to facilitate Zn^{2+} extrusion (Figure 5D). This malfunction of the mutated ZnT-1 is due to a block in the ability to transport zinc *per se*, rather than disruption in its trafficking to the plasma membrane; confocal microscopy shows similar localization of the mutant and the wild type ZnT-1 (Figure 6).

Discussion

ZnT-1 is a multifunctional protein that has three independent roles: 1) Protection of cells from zinc toxicity [11, 17]; 2) Inhibition of the L type calcium channels (LTCC) [23, 33]; and 3) Activation of the Ras-Raf-ERK signal transduction pathway with consequent augmentation of T-type calcium channels and protection of cardiomyocytes against ischemia reperfusion injury [22, 30]. Over the years, studies have provided evidence to support the notion that ZnT-1

acts to extrude zinc from the cell. We have demonstrated, for the first time, that ZnT-1 acts as a Zn^{2+}/H^{+} exchanger, that it is calcium dependent, sodium independent, and, since no LTCC are expressed in HEK293T cells, that efflux of zinc through the activity of ZnT-1 acting as a zinc extruder is responsible for its ability to protect cells against zinc toxicity.

Similar to other zinc extruders, such as the Na^{+}/Zn^{2+} transporter [34], we show that the time course for ZnT-1 mediated zinc extrusion is several tenths of a second (Fig 1A and 1B). Given the large electrochemical gradient for Zn^{2+} ions, the extrusion of zinc from the cytosol to the extracellular compartment requires an energy source to drive Zn^{2+} against this gradient. In mammalian cells, a component of the regulation of intracellular calcium and proton concentrations is mediated primarily by ATPase pumps. Although Zn^{2+}-ATPase pumps have been discovered in bacteria and higher plants [35, 36], no such pump has been described for zinc in mammalian cells. Thus, a secondary active efflux mechanism is the most plausible process for regulating intracellular zinc. Such mechanisms for the extrusion of zinc have been previously described in a variety of cells including epithelia (HEK 293T cells), and cortical neurons [37-40]. Our findings show that ZnT-1 acts as an H^{+}/Zn^{2+}exchanger, catalyzing zinc efflux against a 100-fold transmembrane gradient (Figure 4A). The rapid and active extrusion of zinc is of particular relevance for neurons that are often exposed to short periods of high extracellular zinc and are, thus, susceptible to toxicity following exposure of a few minutes only [41-43]. Hydrogen ions serve as a driving force rather than as modulators of ZnT-1 activity. This is similar to what has been previously shown by Colvin et. al., describing hZIP1 that mediates hydrogen driven zinc uptake [44]. Since ischemia is commonly associated with the development of acidosis in the heart and the brain [45-47], the hydrogen ion dependence of ZnT-1 activity further highlights the adaptation of ZnT-1 to protect against zinc toxicity under pathological situations.

Similarly to other proton-driven secondary active transport systems in mammalian cells the activity of ZnT-1 is sodium independent. The involvement of calcium ions in the activity of ZnT-1 is more complex. A Hill coefficient close to 2, and no effect of magnesium ions on ZnT-1 activity (Fig 2D), are consistent with a specific cooperative action of calcium (Fig 2A and 2C). Calcium may stimulate ZnT-1 activity by modulating an extracellular site. Alternatively, the electrochemical gradient of calcium may serve as an energy source for ZnT-1 activity. However, since little ZnT-1 mediated Zn^{2+} efflux is observed in the presence of calcium and the absence of a pH gradient (Fig 3A), it is unlikely that calcium serves as a driving force. This finding may have pathological significance. During ischemia and rapid

electrical stimulation (such as during a seizure) there is a dramatic decrease in extracellular calcium concentrations [48, 49]. This reduction in extracellular zinc may attenuate Zn^{+2} transport by ZnT-1, leading to increased sensitivity to zinc toxicity during ischemia. Nonetheless, at reperfusion, extracellular calcium concentrations are restored, enabling ZnT-1 to protect cells during this phase.

Despite the modest overall homology between the bacterial YiiP transporter and the ZnT family, a striking overlap exists in their structure. Recent studies shed new light on the organization of the catalytic domain and particularly the four amino acid residues (three of which are highly conserved) composing the binding site for Zn^{2+} [14, 24]. Here we propose a three-dimensional model of the ZnT-1 protein and its zinc binding domain based on the homology between the bacterial CDF, YiiP, and ZnT-1. The validity of our model is supported by the fact that mutation of 2 of the amino acids that are predicted to make up the putative zinc binding domain of ZnT-1 inhibited Zn^{2+} efflux via ZnT-1, leaving the cells susceptible to zinc toxicity (Fig 5).

In summary, this study shows that the underlying mechanism by which ZnT-1 mediates active zinc efflux against its electrochemical gradient is pH-driven and calcium-dependent. Based on a 3D model, we have identified a putative zinc binding domain in ZnT-1 and, by mutating two amino acids within this domain, blocked zinc efflux via ZnT-1. Cellular toxicity caused by zinc accumulation occurs in many pathological conditions, including brain seizures. Seizures are accompanied by acidification and even changes in calcium due to cell damage. The pH and calcium dependency of ZnT-1 mediated Zn^{2+} efflux, therefore, would enhance its ability to protect cells against these noxious conditions.

Acknowledgments

This work was supported by Israel Science Foundation (ISF) 497/11 and the Australian Research Council (ARC) DP130104790.

Figure Legends

Figure 1; ZnT-1 mediates Zn^{2+} efflux: HEK293T cells loaded with FluoZin-3 (A) or Fura-2 (B) were loaded with Zn^{2+} by incubating them in Ringer's solution containing 5 µM Zn^{2+} carrier pyrithione and 1 µM Zn^{2+}. Thereafter, the cells were washed with Ringer's solution

containing 100 µM EGTA. Regions of interest were selected by identifying cells expressing the plasmids prior to the beginning of the experiments. Cells expressing ZnT-1 were identified fluorescently with ZnT-1 tagged with CFP or EYFP for Fluozin-3 and Fura-2 experiments, respectively. Decreasing intracellular Zn^{2+} was observed with either dye only from cells transfected with ZnT-1 plasmid. C. Mean ± SEM summarizing the rate of Zn^{2+} efflux normalized to efflux in ZnT-1-transfected cells. The efflux rate was determined as the initial linear reduction in fluorescence as a function of time and normalized with the rate in ZnT-1 transfected cells. Data are from 10 and 23 slides, each containing 11 regions of interest with at least 10 cells in each region of interest (for pcDNA and ZnT-1 transfected cells, respectively). The rate efflux from ZnT-1 transfected cells is significantly higher than the efflux from control cells (*** $p<0.001$).

Figure 2; ZnT-1 mediated efflux is calcium dependent and sodium independent; A. HEK 293T cells transfected with ZnT-1 plasmid were loaded with Fura-2 and Zn^{2+} as described for figure 1. Consistent with the findings in figure 1, an efflux was observed when the cells were washed with Ringer's solution containing 1mM calcium (CaR-●). In contrast, when calcium was omitted from the medium, no efflux was observed (first part of CaF-■). However, Zn^{2+} efflux was observed when calcium was added back into the wash medium (last part of CaF-■). B. A bar graph showing that the ZnT-1 mediated efflux is sodium independent (sodium was replaced with N-methyl D-glucamine (NMG). C. A bar graph summarizing three independent experiments comparing efflux rates of Zn in the presence of $Ca^{+2,}$, Ca^{+2}+Mg^{+2} and when Mg^{+2} is substituted for Ca^{+2} in the Ringer's solution. D. Cells transfected with ZnT-1 were loaded with Zn^{2+}, as before, and washed with Ringer's solution containing different concentrations of calcium. The data are fitted to a Hill equation yielding a Hill coefficient of 1.7 consistent with a cooperative effect of calcium ions. Data are Mean ± SEM. *** represents $p < 0.001$.

Figure 3; ZnT-1 induced Zn^{2+} efflux is pH dependent; A. Hydrogen ion concentration dependency of ZnT-1 induced Zn^{2+} efflux. HEK 293T cells were loaded with Zn^{2+} as described above. Efflux is plotted as a function of the $[H^+]$ of the superfusing solution. The line through the data points is a fit of the data to a Michaelis Menten equation, yielding an apparent Km of pH=6.8±0.2. B. ZnT-1 induced Zn^{2+} efflux depends upon the H^+ gradient and not on the intracellular pH. Intracellular pH was manipulated by incubating the cells either with 30 mM ammonium chloride (ZnT-1NH_4), thus alkalinizing the cytosol, or with 30 mM butyrate (ZnT-1-butyrate), thus acidifying the cytosol. The superfusing solution was at pH

7.4. Data are from 3 independent experiments and represent Mean ± SEM. * and ** represent $p < 0.05$ and 0.01.

Figure 4; ZnT-1 mediates Zn^{2+} efflux against its electrochemical gradient. A. Changes in intracellular Zn^{2+} as a function of time following washing with zinc containing Ringer's. HEK 293T cells were loaded with Zn^{2+} as described before and washed with Ringer's solution at pH 6.5 containing 10 µM $ZnCl_2$. B. The rate of efflux mediated by ZnT-1 as a function of extracellular Zn^{2+} in the superfusing solution. HEK 293T cells were loaded as described above and efflux was measured in Ringer's solution containing different concentrations of $ZnCl_2$. The line through the data points resulted from fitting the data to an exponential decay equation.

Figure 5; ZnT-1 mediated Zn^{2+} efflux is essential for ZnT-1 to protect cells against zinc Zn^{2+} toxicity. Release of LDH served as a measure for cellular toxicity in HEK 293 cells transfected with mutated, truncated and full length ZnT-1 and exposed to different concentrations of zinc. A. ZnT-1 protects cells against Zn^{2+} toxicity but both ZnT-1 minus its C terminal (ZnTΔCT) and the C terminal by itself (CT) confer no protective properties. B. A 3D homology model in ribbon representation of ZnT-1 is based on the crystal structure of *E. coli* YiiP (3H90). The functional dimer assembly is built from two ZnT-1 monomers (orange and purple) including the membrane zinc binding site (sticks shown in purple). C. Mutating D254A and H43A located in the ZnT-1 putative Zn^{2+} binding site rendered ZnT-1 inactive as a defense against Zn^{2+} toxicity. D. Bar graph showing that ZnT-1 mutated at D254A and H43A blocks the ability of ZnT-1 to mediate Zn^{2+} efflux. Data are Mean ± SEM from 10 slides from 4 independent experiments. *** represents $p < 0.001$.

Figure 6; ZnT-1D254A_H43A localizes to the plasma membrane similarly to wild type ZnT-1: Fluorescence images of HEK 293T cells expressing both ZnT-1 D254A_H43A:EYFP and ZnT-1 WT:ECFP. Images resulting from excitation of the ZnT-1D254A_H43A:EYFP (488 nm laser line), shown in red (A) reveal that it is localized to the cell membrane. Images resulting from excitation of ZnT-1 WT:ECFP (408 nm laser line) shown in blue (B) were segmented and merged to reveal co-localization of mutated ZnT-1 and WT ZnT-1 shown in purple (C) .

References

1. N. Roohani, R. Hurrell, R. Kelishadi and R. Schulin, *Journal of research in medical sciences : the official journal of Isfahan University of Medical Sciences*, 2013, 18, 144-157.
2. T. Kambe, B. P. Weaver and G. K. Andrews, *Genesis (New York, N.Y. : 2000)*, 2008, 46, 214-228.
3. J. Y. Uriu-Adams and C. L. Keen, *Birth defects research. Part B, Developmental and reproductive toxicology*, 2010, 89, 313-325.
4. B. L. Vallee and K. H. Falchuk, *Physiol Rev*, 1993, 73, 79-118.
5. S. Y. Assaf and S. H. Chung, *Nature*, 1984, 308, 734-736.
6. D. Choi and J. Koh, *Annu Rev Neurosci*, 1998, 21, 347-375.
7. C. J. Frederickson, L. J. Giblin, A. Krezel, D. J. McAdoo, R. N. Mueller, Y. Zeng, R. V. Balaji, R. Masalha, R. B. Thompson, C. A. Fierke, J. M. Sarvey, M. de Valdenebro, D. S. Prough and M. H. Zornow, *Exp Neurol*, 2006, 198, 285-293.
8. R. A. Colvin, W. R. Holmes, C. P. Fontaine and W. Maret, *Metallomics*, 2010, 2, 306-317.
9. J.-Y. Koh, S. W. Suh, B. J. Gwag, Y. Y. He, C. Y. Hsu and D. W. Choi, *Science*, 1996, 272, 1013-1016.
10. Y. H. Kim, E. Y. Kim, B. J. Gwag, S. Sohn and J. Y. Koh, *Neuroscience*, 1999, 89, 175-182.
11. T. Kambe, *Biosci Biotechnol Biochem*, 2011, 75, 1036-1043.
12. R. J. Cousins, J. P. Liuzzi and L. A. Lichten, *J Biol Chem*, 2006, 281, 24085-24089 Epub 22006 Jun 24022.
13. R. D. Palmiter and L. Huang, *Pflugers Arch*, 2004, 447, 744-751.
14. T. Kambe, *Curr Top Membr*, 2012, 69, 199-220.
15. L. Huang and S. Tepaamorndech, *Molecular aspects of medicine*, 2013, 34, 548-560.
16. J. Jeong and D. J. Eide, *Molecular aspects of medicine*, 2013, 34, 612-619.
17. R. Palmiter and S. Findley, *EMBO J.*, 1995, 14, 639-649.
18. M. Tsuda, K. Imaizumi, T. Katayama, K. Kitagawa, A. Wanaka, M. Tohyama and T. Takagi, *J. Neurosci.*, 1997, 17, 6678-6684.
19. C. Nolte, A. Gore, I. Sekler, W. Kresse, M. Hershfinkel, A. Hoffmann, H. Kettenmann and A. Moran, *Glia*, 2004, 48, 145.
20. J. D. Park, S. S. Habeebu and C. D. Klaassen, *Toxicology*, 2002, 171, 105-115.
21. C. Urani, P. Melchioretto and L. Gribaldo, *Toxicology in vitro : an international journal published in association with BIBRA*, 2010, 24, 370-374.
22. O. Beharier, S. Dror, S. Levy, J. Kahn, M. Mor, S. Etzion, D. Gitler, A. Katz, A. J. Muslin, A. Moran and Y. Etzion, *J Mol Med (Berl)*, 2012, 90, 127-138 Epub 2011 Dec 2023.
23. O. Beharier, Y. Etzion, A. Katz, H. Friedman, N. Tenbosh, S. Zacharish, S. Bereza, U. Goshen and A. Moran, *Cell Calcium*, 2007, 42, 71-82.
24. E. Ohana, E. Hoch, C. Keasar, T. Kambe, O. Yifrach, M. Hershfinkel and I. Sekler, *J Biol Chem*, 2009, 284, 17677-17686.
25. B. Montanini, D. Blaudez, S. Jeandroz, D. Sanders and M. Chalot, *BMC genomics*, 2007, 8, 107.
26. M. Lu and D. Fu, *Nature Structural Biol*, 2009, 16, 1063-1607.
27. G. Grass, M. Otto, B. Fricke, C. J. Haney, C. Rensing, D. H. Nies and D. Munkelt, *Archives of microbiology*, 2005, 183, 9-18.
28. M. Lu and D. Fu, *Science*, 2007, 317, 1746-1748 Epub 2007 Aug 1723.
29. T. Jirakulaporn and A. J. Muslin, *J Biol Chem*, 2004, 279, 27807-27815.
30. M. Mor, O. Beharier, S. Levy, J. Kahn, S. Dror, D. Blumenthal, L. A. Gheber, A. Peretz, A. Katz, A. Moran and Y. Etzion, *Am J Physiol Cell Physiol*, 2012, 303, C192-203.
31. Schrodinger, LLC, unpublished work.
32. I. Aiba, A. K. West, C. T. Sheline and C. W. Shuttleworth, *Journal of neurochemistry*, 2013, 125, 822-831.

33. S. Levy, O. Beharier, Y. Etzion, M. Mor, L. Buzaglo, L. Shaltiel, L. A. Gheber, J. Kahn, A. J. Muslin, A. Katz, D. Gitler and A. Moran, *J Biol Chem*, 2009, 284, 32434-32443 Epub 32009 Sep 32418.
34. E. Ohana, D. Segal, R. Palty, T. T. Dien, A. Moran, S. L. Sensi, J. H. Weiss, M. Hershfinkel and I. Sekler, *Journal of Biological Chemistry*, 2004, 279, 4278-4284.
35. A. C. Rosenzweig and J. M. Arguello, *Curr Top Membr*, 2012, 69, 113-136.
36. J. Tan, J. Wang, T. Chai, Y. Zhang, S. Feng, Y. Li, H. Zhao, H. Liu and X. Chai, *Plant biotechnology journal*, 2013, DOI: 10.1111/pbi.12027.
37. T. J. Simons, *The Journal of membrane biology*, 1991, 123, 73-82.
38. E. Ohana, D. Segal, R. Palty, D. Ton-That, A. Moran, S. L. Sensi, J. H. Weiss, M. Hershfinkel and I. Sekler, *J Biol Chem*, 2004, 279, 4278-4284.
39. Y. Qin, D. Thomas, C. P. Fontaine and R. A. Colvin, *Journal of neurochemistry*, 2008, 107, 1304-1313.
40. Y. Qin, D. Thomas, C. P. Fontaine and R. A. Colvin, *Neuroscience letters*, 2009, 450, 206-210.
41. C. T. Sheline, M. M. Behrens and D. W. Choi, *J Neurosci*, 2000, 20, 3139-3146.
42. C. J. Frederickson, M. D. Hernandez and J. F. McGinty, *Brain-Res*, 1989, 480, 317-321.
43. S. W. Suh, J. W. Chen, M. Motamedi, B. Bell, K. Listiak, N. F. Pons, G. Danscher and C. J. Frederickson, *Brain research*, 2000, 852, 268-273.
44. R. A. Colvin, *Am J Physiol Cell Physiol*, 2002, 282, C317-329.
45. E. M. Nemoto and S. Frinak, *Stroke; a journal of cerebral circulation*, 1981, 12, 77-82.
46. H. M. Piper, D. Garcia-Dorado and M. Ovize, *Cardiovasc Res*, 1998, 38, 291-300.
47. S. L. Sensi, E. Rockabrand and L. M. Canzoniero, *Biogerontology*, 2006, 7, 367-374.
48. T. Kristian and B. K. Siesjo, *Stroke; a journal of cerebral circulation*, 1998, 29, 705-718.
49. U. Heinemann, A. Konnerth, R. Pumain and W. J. Wadman, *Advances in neurology*, 1986, 44, 641-661.

FIGURE 1

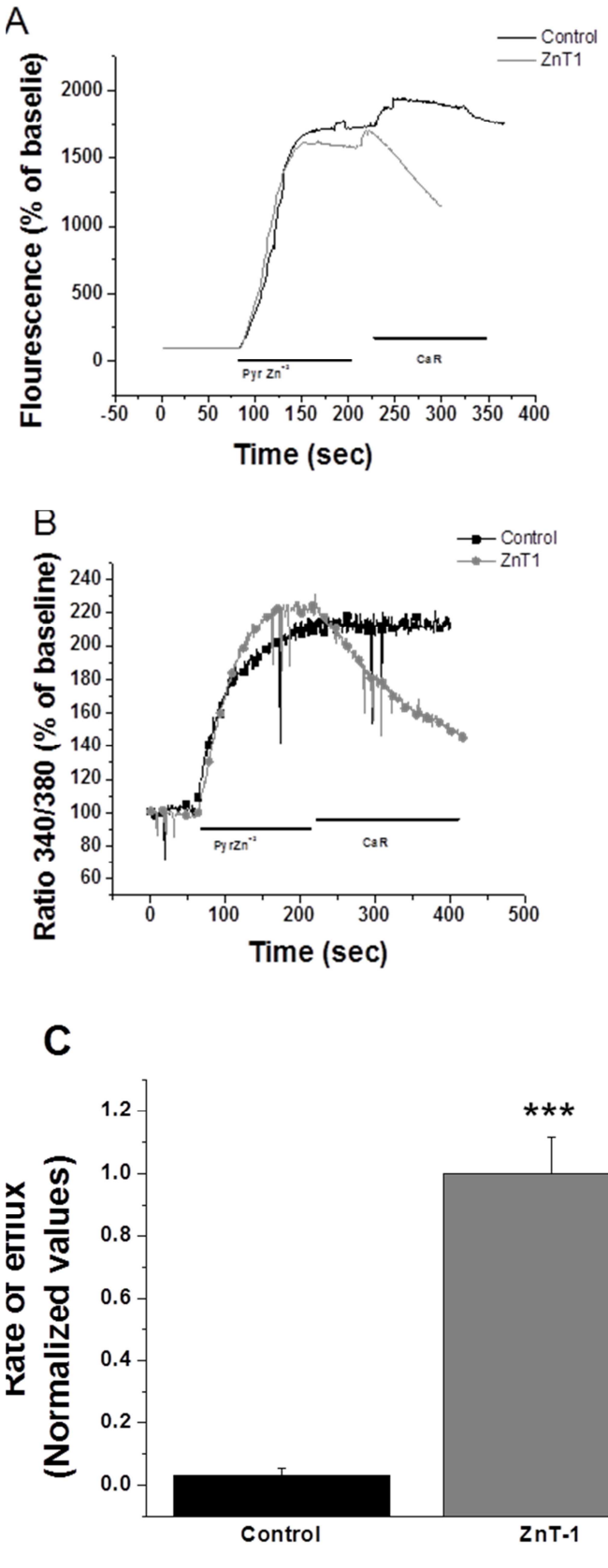

FIGURE 2

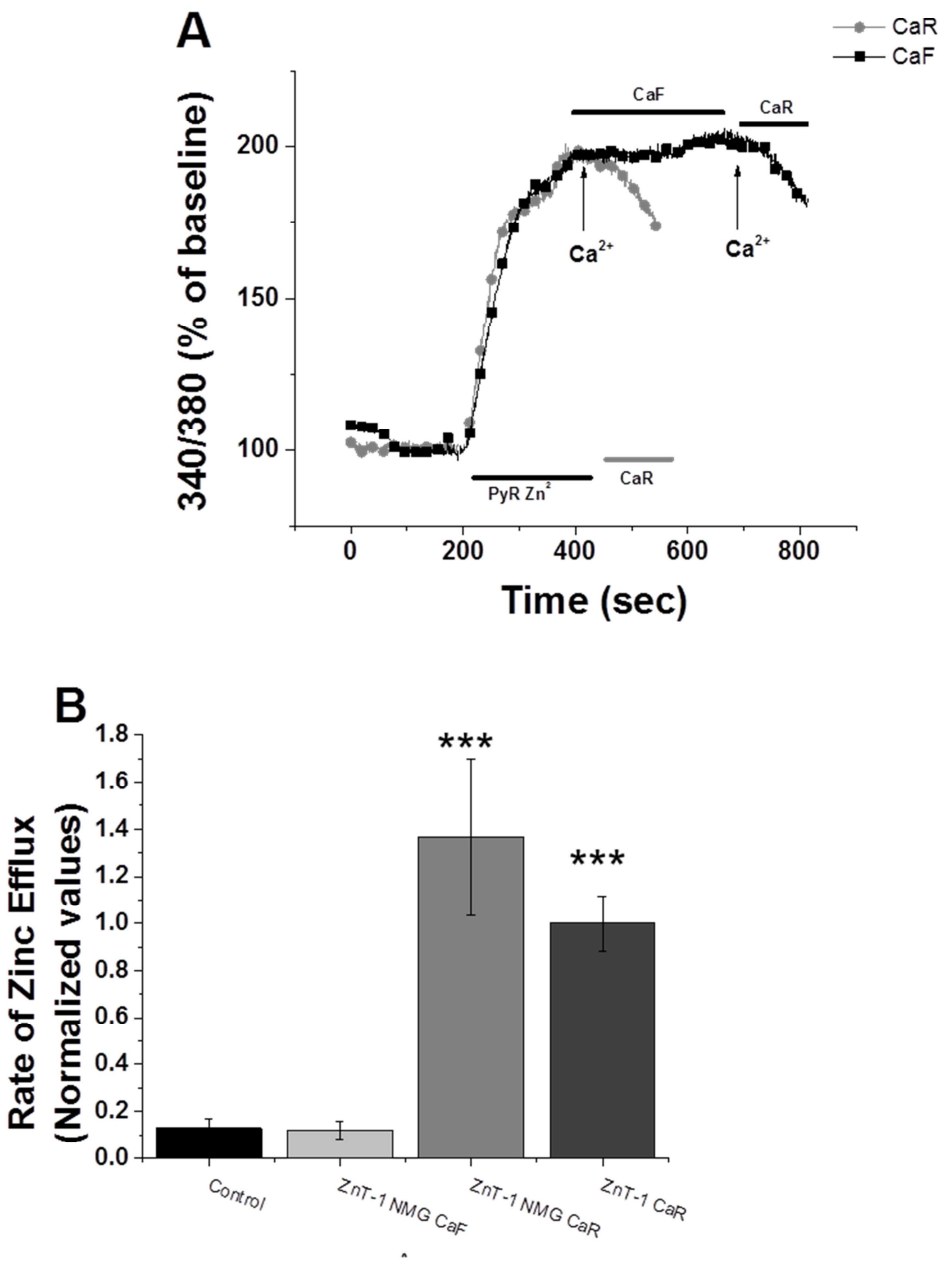

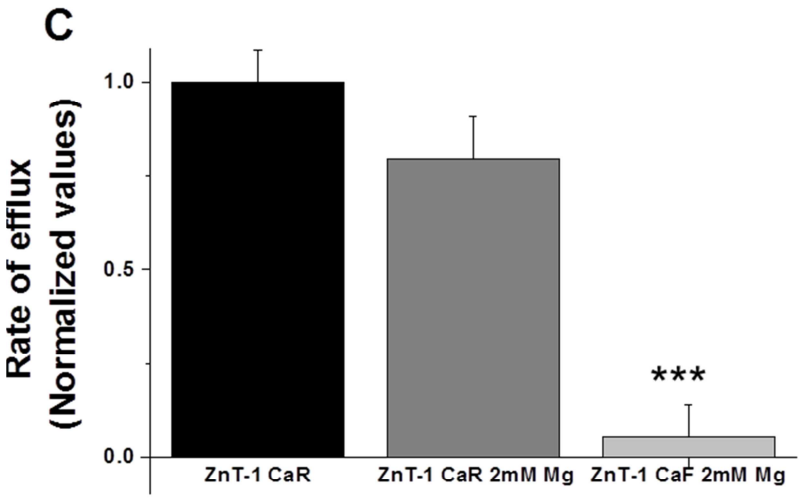

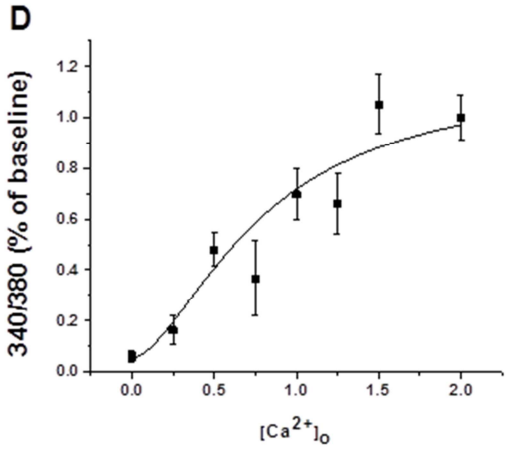

FIGURE 3

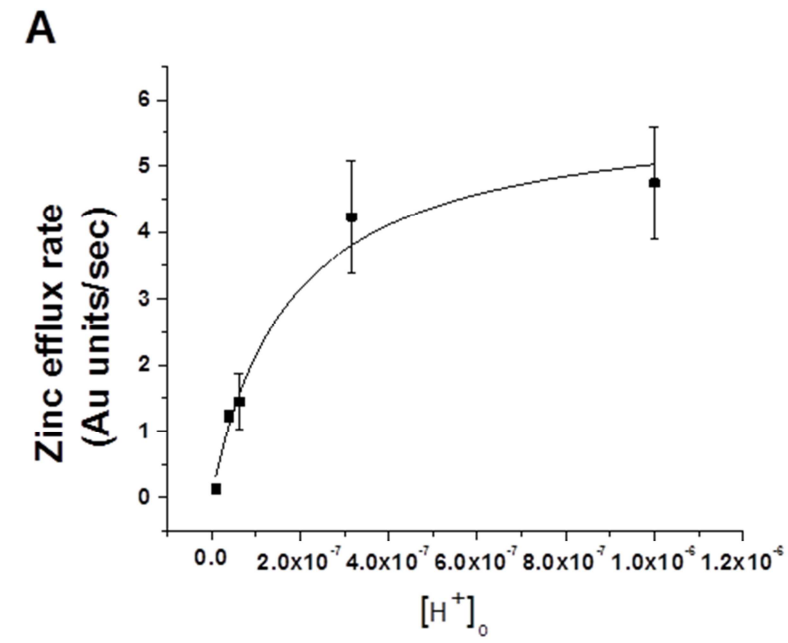

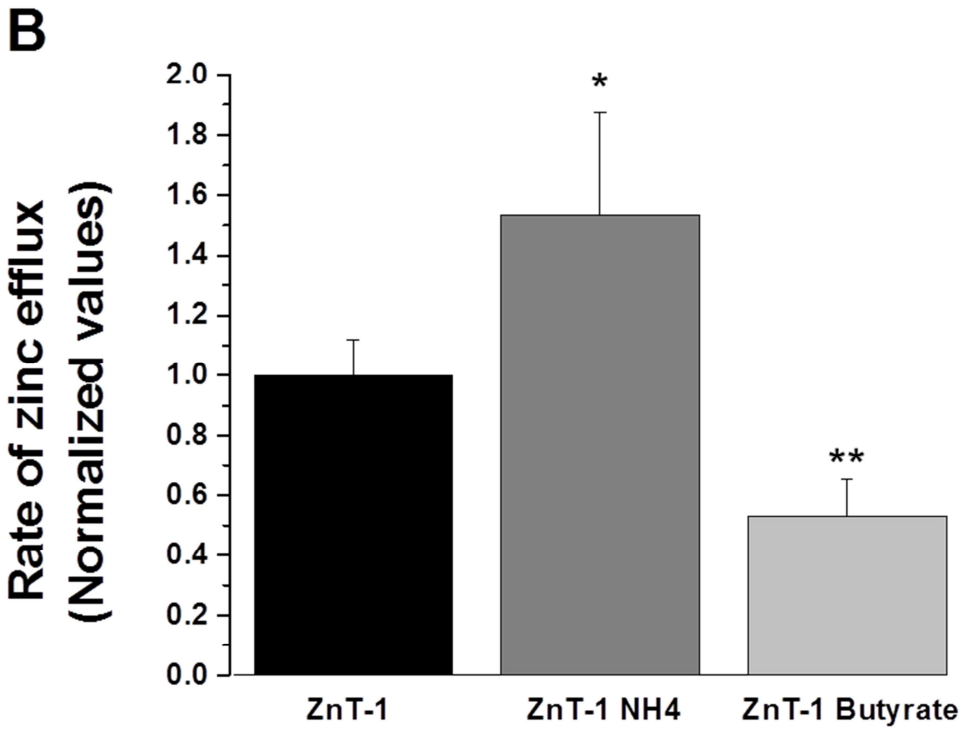

FIGURE 4

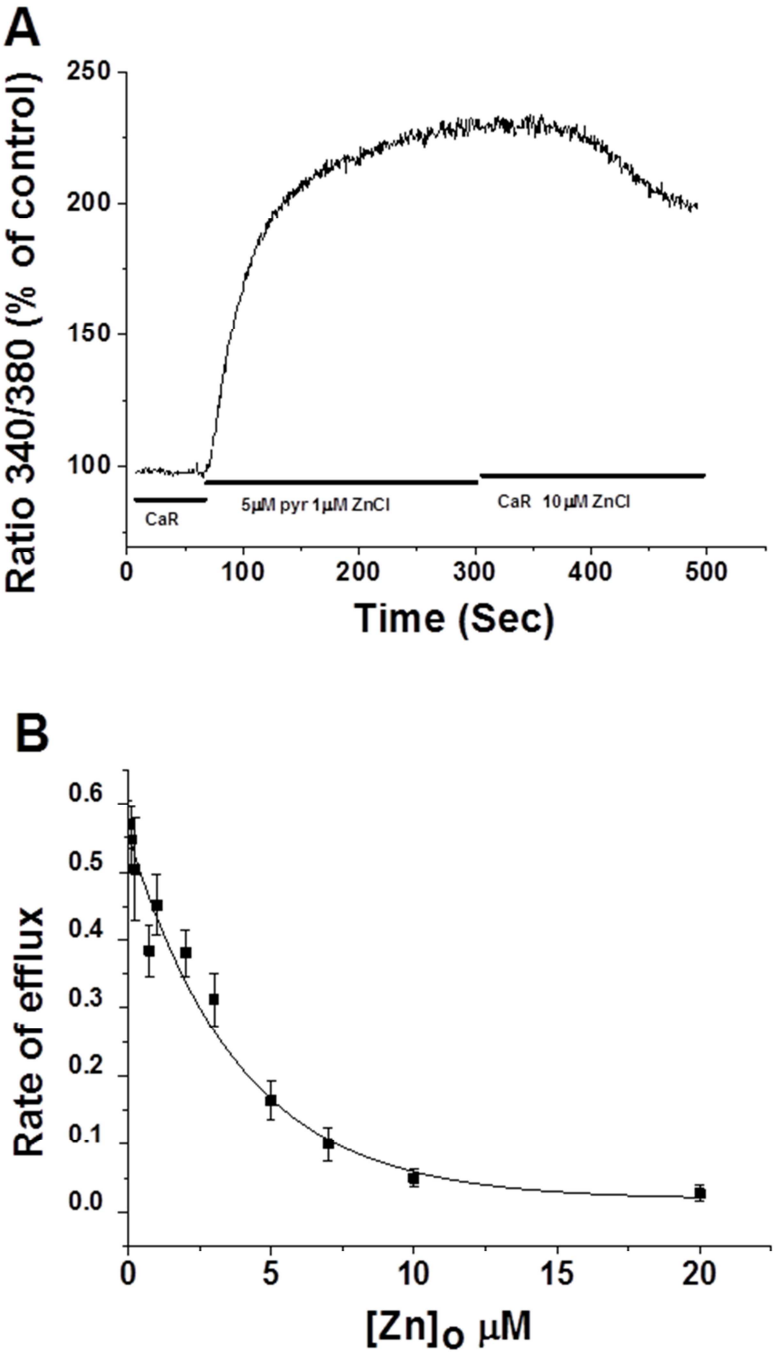

FIGURE 5

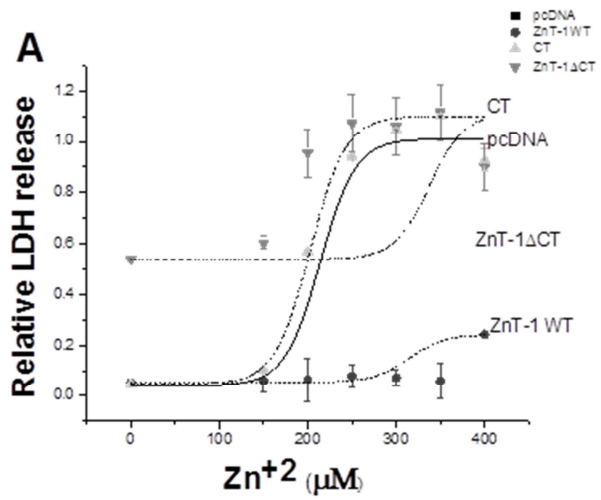

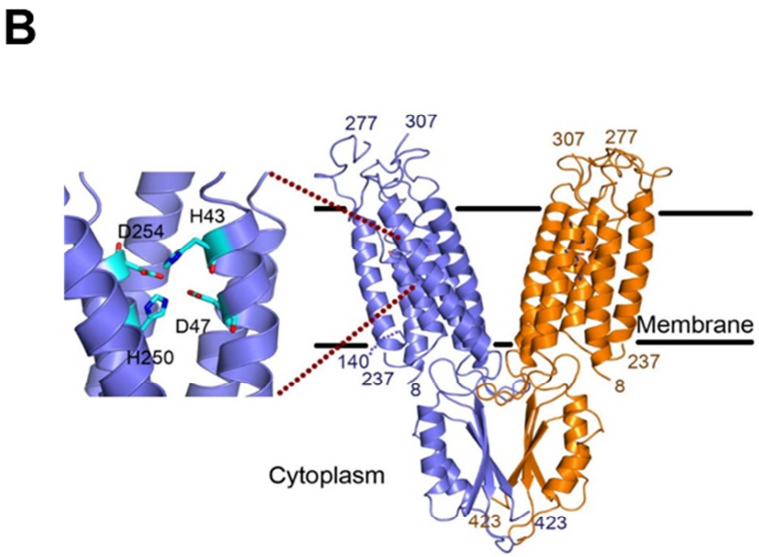

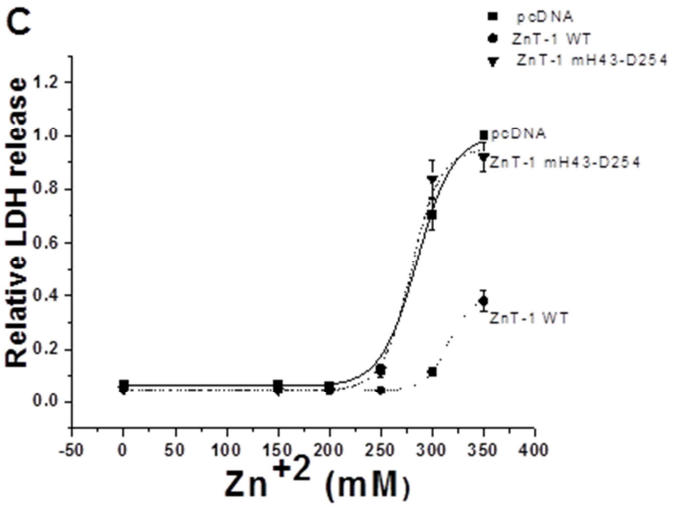

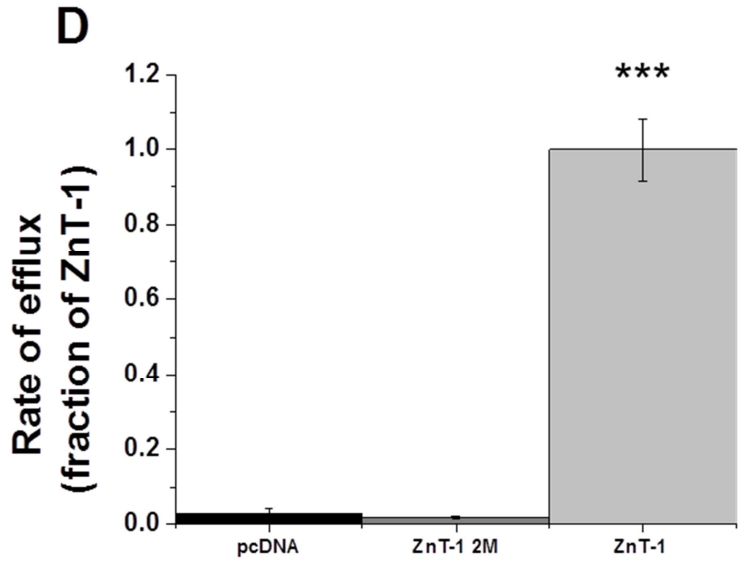

FIGURE S1